Nonlinear atmospheric variability in the winter northeast Pacific associated with the Madden-Julian oscillation

Cédric Jamet and William W. Hsieh

Department of Earth and Ocean Sciences, University of British Columbia, Vancouver, British Columbia, Canada

Received 17 May 2005; accepted 13 June 2005; published XX Month 2005.

Article in Proof

[1] The Madden-Julian Oscillation (MJO), the primary mode of large-scale intraseasonal variability in the tropics, is known to relate to the mid-latitude atmospheric variability. Using neural network techniques, a nonlinear projection of the MJO onto the precipitation and 200-hPa wind anomalies in the northeast Pacific during January–March shows asymmetric atmospheric patterns associated with different phases of the MJO. For precipitation, the strength of the nonlinear effect to the linear effect was 0.94 (in terms of the squared anomalies and averaged over all phases of the MJO), indicating strong nonlinearity, while for the 200-hPa wind, the ratio was 0.55, indicating moderate nonlinearity. In general, anomalous winds blowing from the north or from land were associated with negative precipitation anomalies, while winds from the south or from the open ocean, with positive precipitation anomalies. The nonlinear effects generally induced positive precipitation anomalies during all phases of the MJO.

Citation: Jamet, C., and W. W. Hsieh (2005), Nonlinear atmospheric variability in the winter northeast Pacific associated with the Madden-Julian oscillation, *Geophys. Res. Lett.*, *32*, LXXXXX, doi:10.1029/2005GL023533.

1. Introduction

[2] The Madden-Julian Oscillation (MJO) is the dominant mode of the subseasonal tropospheric variability over the tropical Indian and Pacific Oceans. The MJO was originally identified as a coherent, eastward-propagating perturbation in the tropical sea level pressure, upper level zonal wind and atmospheric convection, with a relatively broad spectral peak of 30–90 days [*Madden and Julian*, 1994]. The impact of the MJO on the atmospheric circulation outside of the tropics has been of considerable interest. There is evidence that deep tropical convection forces the mid-latitude flow both directly [*Hoskins and Karoly*, 1981; *Horel and Wallace*, 1981] and indirectly [*Schubert and Park*, 1991]. Connections have been found between mid-latitude weather variations and the MJO [*Higgins and Mo*, 1997; *Mo and Higgins*, 1998; *Jones*, 2000; *Bond and Vecchi*, 2003, hereinafter referred to as BV]. Most of the studies on the MJO used an index to present and explain the MJO life cycle in the tropics and extratropics. These studies worked with linear methods, e.g. phase sum composite, correlation, regression [*Hendon and Salby*, 1994; *Knutson and Weickmann*, 1987; *Rui and Wand*, 1990; *Maloney and Hartmann*, 1998; BV]. Recently, a multiple linear regression model has been used to analyse the relationships between eastward- and westward-moving intraseasonal modes by *Roundy and Frank* [2004], who concluded that the regression model produced physically valid analyses that revealed processes of partly nonlinear wave interactions in the tropical atmosphere.

[3] In recent years, neural network (NN) methods have been increasingly applied to nonlinearly study the atmosphere and oceans, with reviews given by *Hsieh and Tang* [1998] and *Hsieh* [2004]. In this study, we apply fully nonlinear NN techniques to create a nonlinear composite life cycle and try to separate the linear and nonlinear responses of the atmosphere to the MJO. The association between the MJO and the climate in the northeast Pacific is investigated by applying a nonlinear projection (i.e. nonlinear regression) of the BV MJO index onto the 200-hPa wind and precipitation anomalies during winter (January–March). If x denotes the MJO index and y, the atmospheric response to MJO, the nonlinear response function $y = f(x)$ can be obtained via NN [*Wu and Hsieh*, 2004] (the nonlinear projection by NN is simply called an *NN projection* thereafter). In contrast to the linear projection, the NN projection detects the fully nonlinear atmospheric variability associated with MJO. As the effects of the MJO over northeast Pacific and the northwestern part of North America (esp. western Canada) is not well documented, the purpose of this study is to reveal the nonlinear association between the winter precipitation and 200 hPa wind anomalies in the northeast Pacific and the tropical MJO.

2. Data and Methods

[4] To characterize the state of the MJO, we used the MJO index developed by *Bond and Vecchi* [2003], available for the period from January 1, 1980 to December 31, 2003. This index is composed of an amplitude A and a phase Φ based on the two leading principal components of the intraseasonal 850-hPa zonal wind in the 5°S–5°N band. An MJO event is defined as a period of 30 or more days during which A exceeds 0.7 standard deviation and during which Φ corresponds to eastward propagation for the entire period. In the A and Φ time series, values are only defined during MJO events.

[5] For the variability in northeast Pacific, we examined the daily 200-hPa wind from the NCEP-NCAR extended reanalysis product [*Kalnay et al.*, 1996] and the daily MSU precipitation (both downloadable from http://www.cdc.noaa.gov). The precipitation data, available during 1979–1995, were derived from channel 1 of the microwave sounding unit, which is sensitive to emission by cloud water and rainfall in the lowest few kilometers of the

Copyright 2005 by the American Geophysical Union.
0094-8276/05/2005GL023533$05.00

atmosphere [*Spencer*, 1993]. The MSU precipitation product is only usable over the ocean. For both datasets, the daily climatological means were subtracted from the daily values to yield the anomalies. To obtain intraseasonal anomalies, a Lanczos response bandpass filter with 240 weights and cutoff periods at 35 and 120 days was applied to the wind and precipitation anomalies [*Duchon*, 1979]. We studied the period 1980–1995 during the months January, February and March for both datasets and the MJO index. The analysis was performed only when MJO events were present, thus shrinking the data record to 968 days. Our study is focused on the northeast Pacific area, between 30°N–60°N and 150°W–112.5°W.

[6] After removing the linear trend, a combined principal component analysis (PCA) was used to compress the meridional and zonal wind anomalies, with the 8 leading principal components (PC) (accounting for 95.2% of the variance) retained. For the precipitation anomalies, the 8 leading PCs, accounting for 64.4% of the variance, were retained. Analysis using different number of PCs showed that our results were not sensitive to the number of modes retained as long as 8 or more PCs were used.

[7] The multi-layer perceptron NN model with 1-hidden layer used here has a similar structure to the multivariate nonlinear regression model used for ENSO prediction by our group [*Hsieh and Tang*, 1998]. Here, the NN model has two inputs (predictors) $A \cos \Phi$ and $A \sin \Phi$ (from the MJO index) and 8 output variables (the 8 leading PCs of the 200-hPa wind anomalies or precipitation anomalies). The inputs were first nonlinearly mapped to intermediate variables h_j (called hidden neurons), which were then linearly mapped to the 8 output variables p_k, i.e.

$$h_j = \tanh\left(w_j A \cos \Phi + \hat{w}_j A \sin \Phi + b_j\right),$$

h_j

$$p_k = \sum_j \tilde{w}_{jk} + \tilde{b}_k \,,$$

where $\hat{w}_j$, w_j, $\tilde{w}_{jk}$, b_j and $\tilde{b}_k$ are the model parameters. With enough hidden neurons, the NN model is capable of modeling any nonlinear continuous function to arbitrary accuracy. Starting from random initial values, the NN model parameters were optimized so that the mean square error (MSE) between the 8 model outputs and the 8 observed PCs was minimized. To avoid local minima during optimization [*Hsieh and Tang*, 1998], the NN model was trained repeatedly 25 times from random initial parameters and the solution with the smallest MSE was chosen.

[8] To reduce the possible sampling dependence of a single NN solution, we repeated the above calculation 100 times with a bootstrap approach. A bootstrap sample was obtained by randomly selecting data (with replacement) 968 times from the original record of 968 days, so that on average about 63% of the original record was chosen in a bootstrap sample [*Efron and Tibshirani*, 1993]. The ensemble mean of the resulting 100 NN models was used as the final NN solution, found to be insensitive to the number of hidden neurons, which was varied from 2 to 10 in a sensitivity test. Results from using 4 hidden neurons are presented. For comparison, the linear regression (LR) model is simply

$$p_k = w_k A \cos \Phi + \hat{w}_k A \sin \Phi + b_k \,.$$

3. Results

[9] The output signal from the NN projection is manifested by a surface in the 8 dimensional space spanned by the PCs; in contrast, the linear projection from LR is manifested by a plane in the same 8-D space (not shown). The phase of the MJO was binned into eight equal parts as in BV, phase 1 ($-\pi \leq \Phi < -3\pi/4$), . . ., phase 8 ($3\pi/4 \leq \Phi < \pi$). ~~of~~ the model outputs were computed for each phase bin by averaging all data with Φ falling within a given bin. Also by combining the PCs with their corresponding spatial patterns (the empirical orthogonal functions) yielded the spatial anomalies during each phase of the MJO. The composite spatial anomalies of the 200-hPa wind and precipitation are shown during the 8 MJO phases in Figure 1, where the top two rows are the LR results, the middle two rows, the NN results, and the bottom two rows, the nonlinear residual (i.e. the NN projection minus the LR projection). The corresponding tropical behaviour of the MJO during the 8 phases are shown in Figure 1 of BV. Ocdp.

[10] With the LR projection, the composites for two out-of-phase bins (e.g. bin 1 and 5, 2 and 6, 3 and 7, 4 and 8) gave essentially the same spatial patterns but with oppositely signed anomalies (Figure 1), due to the limitations of the LR method. In contrast, for the NN projection, the patterns and the amplitudes of the 200-hPa wind and precipitation anomalies changed as the phase of the MJO varied across the bins, without showing the strict antisymmetry between two out-of-phase bins. For instance, during phase 1 with LR projection, there is a dipole structure in the precipitation anomalies, with negative anomalies along the coast and positive anomalies further west. The superimposed wind composite shows wind blowing from the land north of 40°N (Figure 1). In the NN projection during phase 1, there is no dipole structure in the precipitation anomalies, but only a large tongue of positive anomalies in the open ocean with a maximum value of 0.7 mm day^{-1}, much greater than the maximum of 0.4 mm day^{-1} found in the LR phase 1 projection. In the NN phase 1, there is an anticyclonic cell over British Columbia, centered just north of Vancouver Island. Generally, over all 8 phases and for both the NN and LR projections, there is quite good agreement between the wind anomalies and the precipitation anomalies (Figure 1), with wind blowing from the north and from land associated with negative precipitation anomalies, and wind blowing from the south and from the open ocean, with positive precipitation anomalies, as expected.

[11] By subtracting the LR projection from the NN projection, the nonlinear residual (bottom two rows of Figure 1) represents the purely nonlinear response after the removal of the linear response. The nonlinear residual for precipitation shows weak nonlinearity during phase 2 and 3 (with maximum anomalies about 0.1 mm day^{-1}) and strong nonlinearity during phase 1, 4 and 5, with anomalies reaching about 0.3 mm day^{-1}. The lack of comparable negative anomalies in the nonlinear residual indicates that

Article in Proof

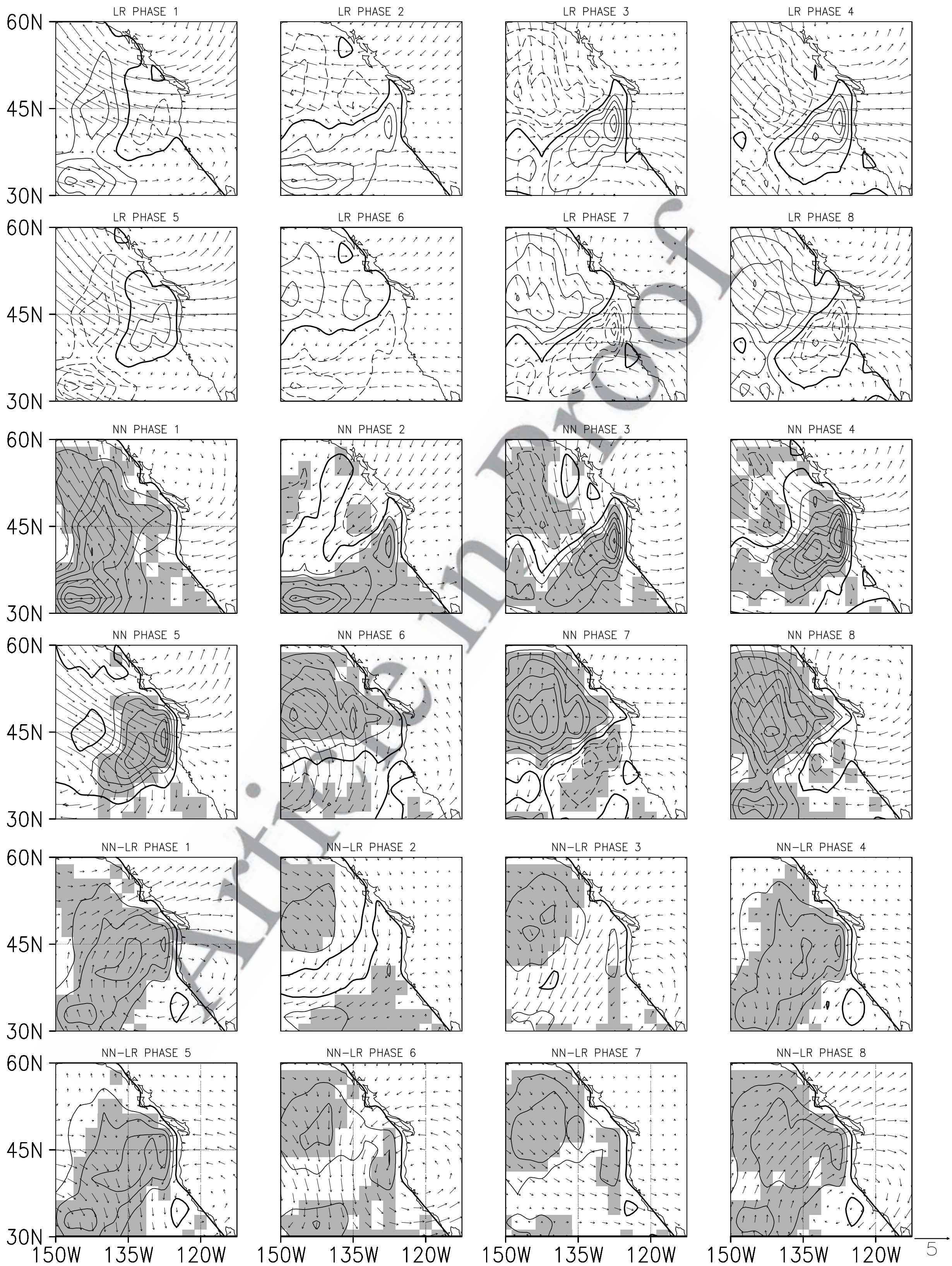

Article in Proof

Figure 1. Composites during the 8 phases of the MJO for the LR projection (top two rows), the NN projection (middle two rows) and the nonlinear residual (NN-LR) (bottom two rows), with precipitation anomalies shown in contour maps and 200-hPa wind anomalies by vectors. With negative contours dashed and zero contours thickened, the contour interval is 0.1 mm day^{-1}, and the scale for the wind (5 m s^{-1}) given beside the bottom right panel. The shaded areas indicate statistical significance for the precipitation anomalies at the 5% level based on the bootstrap distribution.

the nonlinear effects tend to induce positive precipitation anomalies over all phases of the MJO.

[12] We next computed the average of the squared precipitation anomalies in each panel in Figure 1, and let *r* be the ratio between this computed value for the nonlinear residual and that for the LR projection during a given phase. For phase 1 to phase 8, the values of *r* are 1.69, 0.25, 0.26, 1.18, 1.79, 0.86, 0.56 and 0.96, respectively, which supports our claim that nonlinearity is weak during phase 2 and 3, but strong during phase 1, 4 and 5, where *r* actually exceeds 1 in all three phases (meaning that the squared anomalies of the nonlinear residual averaged over the spatial domain exceeds the corresponding value from the linear projection).

[13] For the wind speed anomalies, the *r* values are 0.37, 0.52, 0.69, 0.15, 0.19, 1.74, 0.28 and 0.43 during phase 1 to phase 8, respectively. The nonlinear effect is weakest during phase 4 and 5 and strongest during phase 6, where there is a strong cyclonic cell on the West Coast. Averaged over all 8 phases, *r* is 0.55, versus an average *r* of 0.94 for precipitation. Thus the overall nonlinear effect is stronger in the precipitation than in the wind. We expect precipitation to be more nonlinear than wind, as precipitation depends on temperature and moisture convergence besides wind, and latent heat, which is governed by a step function, introduces strong nonlinearity into precipitation.

4. Conclusion

[14] This study has applied a fully nonlinear technique to study the nonlinear association between the MJO and the northeast Pacific variability of precipitation and 200-hPa wind during January–March. By projecting from the MJO index to the variables in the northeast Pacific, the linear and nonlinear response to MJO were found. For precipitation, the strength of the nonlinear effect to the linear effect was 0.94 (in terms of the squared anomalies and averaged over all phases of the MJO). This means the nonlinear effect was essentially of the same strength as the linear effect. For the 200-hPa wind, the ratio was 0.55, indicating moderate nonlinearity. In general, anomalous winds blowing from the north or from land were associated with negative precipitation anomalies, while winds from the south or from the open ocean, with positive precipitation anomalies. The nonlinear effects generally induced positive precipitation anomalies during all phases of the MJO. Follow-on work could further explore time lags between MJO and variables in the northeast Pacific.

[15] **Acknowledgments.** The authors would like to thank Dr. Gabriel Vecchi for providing his MJO index, and Drs. Phil Austin and Aiming Wu for their useful comments. The authors acknowledge the support from the Natural Sciences and Engineering Research Council of Canada via research and strategic grants.

References

Bond, N. A., and G. A. Vecchi (2003), The influence of the Madden-Julian oscillation on precipitation in Oregon and Washington, *Weather Forecasting*, *18*, 600–613.

Duchon, C. E. (1979), Lanczos filter in one and two dimensions, *Appl. Meteorol.*, *18*, 1016–1022.

Efron, B., and R. J. Tibshirani (1993), *An Introduction to the Bootstrap*, CRC Press, Boca Raton, Fla.

Hendon, H. H., and M. L. Salby (1994), The life cycle of the Madden-Julian oscillation, *J. Atmos. Sci.*, *51*, 2227–2240.

Higgins, R. W., and K. C. Mo (1997), Persistent North Pacific circulation anomalies and the tropical intraseasonal oscillation, *J. Clim.*, *10*, 223–244.

Horel, J. H., and J. M. Wallace (1981), Planetary scale atmospheric phenomenon associated with the Southern Oscillation, *Mon. Weather Rev.*, *109*, 813–829.

Hoskins, B. J., and D. J. Karoly (1981), The steady linear response of a spherical atmosphere to thermal and orographic forcing, *J. Atmos. Sci.*, *38*, 1179–1196.

Hsieh, W. W. (2004), Nonlinear multivariate and time series analysis by neural network methods, *Rev. Geophys.*, *42*, RG1003, doi:10.1029/2002RG000112.

Hsieh, W. W., and B. Tang (1998), Applying neural network models to prediction and data analysis in meteorology and oceanography, *Bull. Am. Meteorol. Soc.*, *79*, 1855–1870.

Jones, C. (2000), Occurrence of the extreme precipitation events in California and relationships with the Madden-Julian oscillation, *J. Clim.*, *13*, 3576–3587.

Kalnay, E., et al. (1996), The NCEP/NCAR 40-Year Reanalysis project, *Bull. Am. Meteorol. Soc.*, *77*, 437–471.

Knutson, T. R., and K. M. Weickmann (1987), 30–60 day atmospheric oscillations: Composite life of convection and circulation anomalies, *Mon. Weather Rev.*, *115*, 1407–1436.

Madden, R. A., and P. R. Julian (1994), Observations of the 40–50 day tropical oscillation—A review, *Mon. Weather Rev.*, *122*, 814–837.

Maloney, E. D., and D. L. Hartmann (1998), Frictional moisture in a composite life cycle of the Madden-Julian oscillation, *J. Clim.*, *11*, 2387–2403.

Mo, K. C., and R. W. Higgins (1998), Tropical convection and precipitation regime in the western United States, *J. Clim.*, *11*, 2404–2423.

Roundy, P. E., and W. M. Frank (2004), Applications of a multiple linear regression model to the analysis of relationships between eastward- and westward-moving intraseasonal modes, *J. Atmos. Sci.*, *61*, 3041–3048.

Rui, H., and B. Wand (1990), Development characteristics and dynamic structure of tropical intraseasonal convection anomalies, *J. Atmos. Sci.*, *47*, 357–379. g/

Schubert, S. D., and C.-K. Park (1991), Low-frequency intraseasonal tropical extratropical interactions, *J. Atmos. Sci.*, *48*, 629–650.

Spencer, R. W. (1993), Global ocean precipitation from the MSU during 1979–1991 and comparisons to other climatologies, *J. Clim.*, *6*, 1301–1326.

Wu, A., and W. W. Hsieh (2004), The nonlinear Northern Hemisphere winter atmospheric response to ENSO, *Geophys. Res. Lett.*, *31*, L02203, doi:10.1029/2003GL018885.

W. W. Hsieh and C. Jamet, Department of Earth and Ocean Sciences, University of British Colombia, 6339 Stores Road, Vancouver, BC, Canada V6T 1Z4. (whsieh@eos.ubc.ca; cjamet@eos.ubc.ca)

Article in Proof